699. Modeling wave propagation through an analytical surface model

J. I. Real [a], C. Zamorano [b], L. Montalbán [a]
[a]Department of Transportation Engineering and Infrastructures, School of Civil Engineering, Technical University of Valencia, 14 Camino de Vera, 46022 Valencia, Spain
[b]Foundation for the Research and Engineering in Railways, 160 Serrano, 28002 Madrid, Spain
E-mail: *jureaher@tra.upv.es, claraz@fundacioncdh.com, laumondo@cam.upv.es*

(Received 17 October 2011; accepted 4 December 2011)

Abstract. Nowadays there is a certain development in the use of railway, especially in the form of trams and underground lines in urban areas. Despite its many advantages, this kind of transport is a significant source of vibrations, which may affect residents and buildings near to the track. Wave transmission through the ground is therefore a phenomenon of particular interest. The object of this article is to formulate and test an analytical model of vibration propagation through the terrain surface. The model is based on the wave equation and takes into account wave scattering and reflection in the interfaces between different soil layers. A sensitivity analysis of its main parameters is carried out, and then a comprehensive set of simulations is made to test model performance and analyze factors such as load magnitude and velocity or soil configuration. The model has proved to be an interesting instrument to study the vibration phenomenon from a theoretical point of view and some improvements are proposed to turn it into a tool for engineers and designers.

Keywords: ground vibrations, tram, wave reflection, convolution.

NOMENCLATURE

a	Track gauge
A_0	First Pandolfo coefficient
A_I	Incoming wave amplitude
A_R	Reflected wave amplitude
A_T	Transmitted wave amplitude
b_n	Fourier coefficients
B_0	Second Pandolfo coefficient
C	Equivalent ballast coefficient
E	Rail Young modulus
g	Wave function for convolution
G	Convolution
I	Rail inertia in y-axis direction
k_i^n	Wave number for each material and harmonic
P	Load function
Q	Static load
R	Distance between the load and the modeling point
R_a	Distance from the rail to the first interface
R_b	Distance from the rail to the second interface
ΔR	Difference between R_a and R_b
s_0	Initial load position
T	Vibration period
u_1	Plane wave in soil 1
u_2	Plane wave in soil 2
v_I	Incoming wave
v_R	Reflected wave

v_T	Transmitted wave
V	Load velocity
V_i	Wave velocity for each material
x_0	X coordinate of the modeling point
y_0	Y coordinate of the modeling point
z_0	Displacement under the rail
z_1	Displacement under the rail considering Pandolfo's theory
z_1^F	Displacement under the rail expressed as a Fourier series
η	Displacement under the rail replicated through point reflection
μ_i	Shear Modulus for each material
$\mu\mu_i$	Damping for each material
ρ_i	Density for each material
k_i^n	Wave damping for each material and harmonic
$\Delta\tau$	Time discretisation
τ_0	Time first limit for the convolution
τ_1	Time second limit for the convolution
ϖ^n	Angular frequency for each harmonic

1. INTRODUCTION

At present there is a growing need for public transport in many cities around the world. Denser and more efficient transport networks are required not only to connect rising populations but to reduce the use of private transport and thus alleviate CO_2 emissions. Urban railways (trams and undergrounds) are a good solution for urban transport needs as they combine high capacity and reliance with low environmental impact.

However, as any other transport mean, trams and undergrounds are the source of certain externalities, which should be addressed in order to avoid negative effects in the environment. One of the most important side effects caused by trams are vibrations, which are transmitted through the track and the ground to the buildings nearby and are potentially damaging to foundations and a source of nuisance for residents.

The phenomenon of wave generation and transmission is still not fully understood despite the comprehensive study and modeling carried out over the last years. The vibration spreading through rather heterogeneous, anisotropic soils is of particular interest so as to assess the effects the wave may have on buildings foundations.

Within this framework the present paper aims to develop a theoretical model of the wave surface transmission through different materials, paying special attention to wave attenuation, reflection and scattering. The main objectives are to formulate the model equations, tests its performance regarding the aforementioned phenomena and propose new ways of research and improvement for the model.

The paper is structured as follow: Firstly, a literature review is developed, covering the main pieces of work and conclusions already established about the topic. Secondly, the model is fully explained, considering its main hypothesis, input, equations and output. Then the model is used to simulate different situations, soils and load inputs to assess its performance. Finally, conclusions and lines of further research are proposed.

2. LITERATURE REVIEW

The problem of modeling vibrations caused by railways has been addressed in many different ways over recent years. There are quite comprehensive pieces of work about the topic such as the ones published by Thompson [1]. Particularly, the generation of vibrations in the

wheel-rail contact and the wave transmission through the track infrastructure has been widely studied (Galvín and Domínguez [2], Metrikine and Vrouwenvelder [3], Salvador et al. [4], Real et al. [5]).

Two main mathematical approaches can be defined for vibration modeling: numerical and analytical. The former has the advantage of being quite adaptable to different track configurations as well as allowing the introduction of localized factors (e.g. track joints, ground irregularities). Examples of numerical modeling can be found in Sheng et al. [6] and Yang et al. [7], whose works rely on Finite Elements Methods (FEM). Other common numerical formulations are Boundary Elements Method (BEM) such as the ones used by Galvín and Domínguez [2] and Celebi [8] as well as Finite Difference Methods (FDM) as found in Katou et al. [9].

Analytical modeling has the main advantage of providing sound physical consistency as well as a continuous solution in the model domain. Therefore, despite their lack of flexibility when compared to numerical models they are more reliable in terms of physical and mathematical coherence. This is the reason that supports the choice of analytical modeling for this paper.

Examples of analytical models of vibration generation in railway tracks can be found in Metrikine and Vrouwenvelder [3], Koziol et al. [10], Salvador et al. [4] and Real et al. [5].

In comparison with vibration generation, the process of wave transmission from the infrastructure and through the ground has not been addressed to the same extent, particularly with respect to application of analytical models. Numerical models such as FEM can reproduce the wave but they usually do not model phenomena such as wave scattering. In addition, the frequency range modeled strongly depends on the domain meshing (Andersen and Nielsen [11]). These features also endorse the choice made.

The model presented in this paper relies on some previous works that also tried to develop a theoretical formulation of wave propagation. Among these it is worth mentioning the studies of Dawn and Stanworth [12] and Gutowski and Dym [13] or, more recently, Jones et al. ([14] and [15]) or Auersch [16]. Of particular interest is the work of Barber [17], whose approach for the convolution has been used as a base for the formulation explained in the paper.

3. METHODOLOGY

In this section the model formulation is thoroughly explained. The model relies on the hypothesis of isotropy and elasticity of the domain considered. This domain is a 2D surface over a half-space (Boussinesq half-space) as shown in Figure 1. A concrete slab track typology is assumed at this stage of research, and thus the modeled surface has three different areas corresponding to the concrete slab and two different soils.

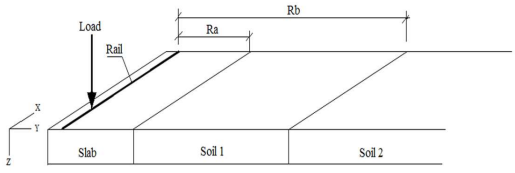

Fig. 1. Model domain

Once formulated, the model is able to provide vertical displacements at any location of the surface, and takes into account wave scattering and reflection at the interfaces between different materials.

3. 1. Model input

The model input is a single point load moving at constant speed V along the concrete slab. This load represents a single train axle. The vertical displacement right under the load is obtained through the Zimmerman method (1):

$$z_0(x) = \frac{Q}{2bC}\sqrt[4]{\frac{aC}{4EI}}e^{-\frac{x}{L}}(\cos\frac{x}{L}+\sin\frac{x}{L}) \quad (1)$$

where Q is the applied load, a the track gauge, E the Young's modulus of the track, I the inertia of the rail, C an equivalent ballast coefficient for the material under the line, and L is an elastic length defined as:

$$L = \sqrt[4]{\frac{4EI}{aC}} \quad (2)$$

Equation (1) can be expressed as a function of time, considering speed V for the load so that $x = Vt$. It is also modified considering the theory of Pandolfo so that load distribution along the track is taken into account. Those changes yield the following equation:

$$z_1(x,t) = z_0(0)\cdot A_0 \cdot e^{-B_0\cdot(x-Vt)^2} \quad (3)$$

where A_0 and B_0 are Pandolfo's coefficients. This deformation under the load generates a wave moving across the whole surface. The wave-front is cylindrical according to Barber [17], whose centre is the moving load. When modeling the displacement at a single point of the surface, it must be taken into account that the distance between that point and the moving load varies with time according to equation (4), as shown in Figure 2.

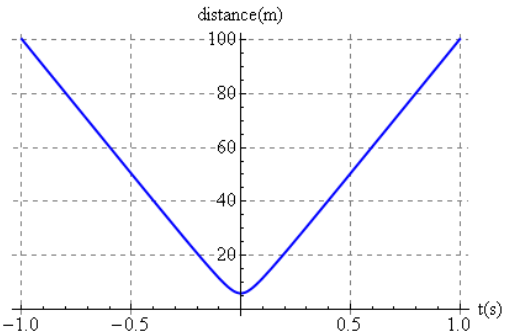

Fig. 2. Variation of distance between the moving load and a point located at 6 meters from the track

$$R(t) = \sqrt{(x_0 - s_0 - V\cdot t)^2 + y_0^2} \quad (4)$$

where s_0 is the position of the load in the initial time, while x_0 and y_0 are the coordinates of the location where vertical displacements would be calculated.

The displacement defined by (3) is then developed as a Fourier series in terms of sinus. In order to ensure that the series is equal to zero at $t = 0$, the displacement is replicated through point reflection (central symmetry) for $t < 0$ by means of equation (5). This is shown in Figure 3.

$$\eta(t) = y_1(0, t-t') - y_1(0, t+t') \quad (5)$$

where t' is the time between 0 and the peak of displacement.

The Fourier coefficients are calculated according to the following equation:

$$b_n = \frac{2}{T}\int_0^T \eta(t)\cdot\sin(\frac{\pi\cdot t\cdot n}{T})dt \quad (6)$$

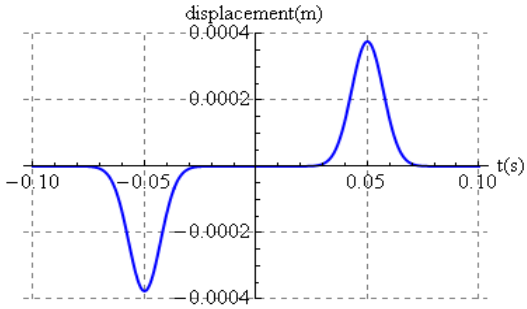

Fig. 3. Displacement replicated through point reflection for $t < 0$

And the displacement under the load is then perfectly defined by the following Fourier series:

$$z_1^F(t) = \sum_{n=1}^{N} b_n \sin(\frac{\pi \cdot t \cdot n}{T}) \tag{7}$$

3. 2. Model core

For each of the three different materials defined in the model domain the following mechanical characteristics are defined:

ρ_i = Density in kg/m^3. i = 0, 1, 2
μ_i = Shear Modulus (G) in Pa. i = 0, 1, 2
$\mu\mu_i$ = Damping in kg/m·s. i = 0, 1, 2

where 0 stands for the concrete slab, 1 for the first layer of soil and 2 for the second one.

If damping in all three materials is assumed to be null, wave velocity is a constant for each material:

$$V_i = \sqrt{\frac{\mu_i}{\rho_i}} \qquad i = 0, 1, 2 \tag{8}$$

and the wave number for each material and harmonic (n) is:

$$k_i^n = \frac{\omega^n}{V_i} \qquad n = 1...N \tag{9}$$

being k^n the angular frequency ($\frac{\pi \cdot n}{T}$) in rad/s for each harmonic.

However, if the damping is not null, wave velocity is no longer constant but depends on the wavelength (wave scattering). Therefore, assuming that T (vibration period) is the same in any case, for whatever material, the wave number for each material and harmonic is as follows (see Udías [18] for more details):

$$k_1^n = \sqrt{2}\sqrt{\frac{\mu_1 \cdot \rho_1}{\mu\mu_1^2} - \frac{\sqrt{(\mu_1^2 - (\omega^n)^2 \cdot \mu\mu_1) \cdot \rho_1}}{\mu\mu_1^2}} \tag{10}$$

$$k_2^n = \sqrt{\frac{2\mu_2 \cdot \rho_2}{\mu\mu_2^2} - \frac{\sqrt{\rho_2^2 \cdot \rho_1^2 \cdot ((k_1^n)^4 \cdot \mu\mu_2^2 \cdot \mu\mu_1^2 - 4(k_1^n)^2 \cdot \mu_1 \cdot \mu\mu_2^2 \cdot \rho_1 + 4\mu_2^2 \cdot \rho_1^2)}}{\mu\mu_2^2 \cdot \rho_1^2}} \tag{11}$$

$$k_0^n = \sqrt{\frac{2\mu_0 \cdot \rho_0}{\mu\mu_0^2} - \frac{\sqrt{\rho_0^2 \cdot \rho_1^2 \cdot ((k_1^n)^4 \cdot \mu\mu_0^2 \cdot \mu\mu_1^2 - 4(k_1^n)^2 \cdot \mu_1 \cdot \mu\mu_0^2 \cdot \rho_1 + 4\mu_0^2 \cdot \rho_1^2)}}{\mu\mu_0^2 \cdot \rho_1^2}} \tag{12}$$

$$n = 1...N$$

and wave velocities are:

$$V_i^n = \sqrt{\frac{\mu_i}{\rho_i} - (\frac{k_i^n \cdot \mu\mu_i}{2\rho_i})^2} \qquad n = 1...N \qquad i = 0, 1, 2 \tag{13}$$

In this case, as the material damping is not null, the wave damping for materials 1 and 2 is as follows:

$$\xi_i^n = \frac{(k_i^n)^2 \cdot \mu\mu_i}{2\rho_i} \qquad n = 1...\mathrm{N} \qquad i = 1, 2 \tag{14}$$

Once these variables are defined for both the damped and undamped case, wave equations are formulated taking into account that when the incoming wave (sub index *I*) reaches the interface between materials 1 and 2 part of it is transmitted (sub index *T*) and part is reflected (sub index *R*). Therefore, wave amplitudes for *I*, *T* and *R* wave need to be formulated separately:

$$A_I(j,n) = \begin{cases} 1 & if \quad k_1^n = k_2^n \quad and \quad j = 0 \\ (\frac{k_1^n - k_0^n}{k_1^n + k_0^n} \cdot \frac{k_1^n - k_2^n}{k_1^n + k_2^n})^j \end{cases} \tag{15}$$

$$A_R(j,n) = \begin{cases} 0 & if \quad k_1^n = k_2^n \quad or \quad k_1^n = k_0^n \quad and \quad j = 1 \\ \frac{k_1^n - k_2^n}{k_1^n + k_2^n} \cdot (\frac{k_1^n - k_0^n}{k_1^n + k_0^n} \cdot \frac{k_1^n - k_2^n}{k_1^n + k_2^n})^{j-1} \end{cases} \tag{16}$$

$$A_T(j,n) = \begin{cases} 1 & if \quad k_1^n = k_2^n \quad or \quad k_1^n = k_0^n \quad and \quad j = 1 \\ 2\frac{k_1^n}{k_1^n + k_2^n} \cdot (\frac{k_1^n - k_0^n}{k_1^n + k_0^n} \cdot \frac{k_1^n - k_2^n}{k_1^n + k_2^n})^{j-1} \end{cases} \tag{17}$$

and the wave equations are:

$$v_I(r,t,n) = [\sum_{j=1}^{4} A_I(j,n) \cdot b_n \cdot \sin(\omega_n(t - \frac{2 \cdot j \cdot \Delta R}{V_1^n} - \frac{r - R_a}{V_1^n})) \cdot e^{-\xi_1^n (t - \frac{2 \cdot j \cdot \Delta R}{V_1^n})}$$
$$\cdot (H(t - \frac{2 \cdot j \cdot \Delta R}{V_1^n} - \frac{r - R_a}{V_1^n}) - H(t - \frac{2 \cdot j \cdot \Delta R}{V_1^n} - \frac{r - R_a}{V_1^n} - 2t'))] \cdot (H(r - R_a) - HT(r - R_b)) \tag{18}$$

$$v_R(r,t,n) = [\sum_{j=1}^{4} A_R(j,n) \cdot b_n \cdot \sin(\omega_n(t - \frac{2 \cdot j \cdot \Delta R}{V_1^n} + \frac{r - R_a}{V_1^n})) \cdot e^{-\xi_1^n (t - \frac{2 \cdot (j-1) \cdot \Delta R}{V_1^n})}$$
$$\cdot (H(t - \frac{2 \cdot j \cdot \Delta R}{V_1^n} + \frac{r - R_a}{V_1^n}) - H(t - \frac{2 \cdot j \cdot \Delta R}{V_1^n} + \frac{r - R_a}{V_1^n} - 2t'))] \cdot (H(r - R_a) - HT(r - R_b)) \tag{19}$$

$$v_T(r,t,n) = [\sum_{j=1}^{4} A_T(j,n) \cdot b_n \cdot \sin(\omega_n(t - \frac{2 \cdot (j-1) \cdot \Delta R}{V_1^n} - \frac{r - R_b}{V_2^n})) \cdot e^{-\xi_2^n \cdot t + (\xi_2^n - \xi_1^n) \cdot \frac{2 \cdot (j-1) \cdot \Delta R}{V_1^n}}$$
$$\cdot (H(t - \frac{2 \cdot (j-1) \cdot \Delta R}{V_1^n} + \frac{r - R_b}{V_2^n}) - H(t - \frac{2 \cdot (j-1) \cdot \Delta R}{V_1^n} + \frac{r - R_b}{V_2^n} - 2t'))] \cdot H(r - R_b) \tag{20}$$

where *r* is the variable of distance between the load and the point of modeling, R_a and R_b are the distances from the rail to each interface between materials; ΔR is the difference between R_a and R_b. The function $H(t)$ is the Heaviside step function (with $H(0) = 1$) and $HT(t)$ is the same function not defined at $t = 0$. These functions are used to ensure that each wave only takes place in the proper place and time of the modeled domain.

Finally, two wave equations are defined for soils 1 and 2 respectively. The first one is the sum of the incoming and reflected wave while the other one is just the transmitted wave. Both equations are divided by *r* to shift these linear waves to plane waves:

$$u_1(r,t,n) = \frac{v_I + v_R}{r} \tag{21}$$

$$u_2(r,t,n)=\frac{v_T}{r} \tag{22}$$

3. 3. Convolution and output

The waves already formulated are the result of a single wave front caused by the point load at a certain position. In order to take into account the full effect of the load when it moves along the track a convolution is made with respect to time and distance.

The functions to be convoluted are the following:

$$P(t) \tag{23}$$

$$g(r,t,\tau)=\begin{cases}u_1(r,t-\tau) & if \quad r<R_b\\ u_2(r,t-\tau) & if \quad r\geq R_b\end{cases} \tag{24}$$

The first one (23) represents the load as a generic function of time in order to give the following process a more general scope. However, in terms of the calculations made in this paper, the load is assumed to be a constant value $P(t) = Q$ as defined for (1) unless stated otherwise. The second equation (24) defines which wave equation is used depending on the location of the point to be analyzed within the model domain.

A discrete convolution of those two functions is then defined (See Barber [17] and Tijonov and Samarsky [19] for more details):

$$G(t)=\Delta\tau\cdot\sum_{\tau 0}^{\tau 1}\left(\frac{P(\tau)}{Q}\right)g(R(\tau),t,\tau) \tag{25}$$

where $\Delta\tau$ is the time discretisation, τ_0 and τ_1 are the limits of the convolution and $R(\tau)$ is the previously defined function (4), which marks the distance between the moving load and the point of analysis with respect to time. Therefore, the convolution (25) allows obtaining the summation of all the wave fronts generated by a moving, variable point load at a single location of the model domain defined by (4). The convolution parameters (τ_0 and τ_1) define the time interval, which should be long enough to cover the whole movement of the point load within the domain. The parameter $\Delta\tau$, in turn, defines the exactitude of the discrete convolution.

4. MODEL PERFORMANCE

In this section a sensitivity analysis of the model is carried out with respect to certain parameters such as the convolution time, discretisation and damping coefficients. Afterwards, a simulation runs are performed with different materials and loads in order to test model performance. The results are then discussed.

First of all the model parameters and variables are fixed to certain reasonable values as shown in Table 1. Then each of all these magnitudes is modified in the following sections.

Table 1. Model parameters and variables

Parameter/variable	SLAB	SOIL 1	SOIL 2
ρ_i (kg/m^3)	*2400*	*1800*	*2000*
μ_i (Pa)	*14E8*	*1.8E8*	*14E8*
$\mu\mu_i$ kg/m·s	*15000*	*5000*	*7000*
MODEL GEOMETRY			
R_a (m)	*2*	R_b (m)	*10*
Thickness (m)	*0.5*		
APPLIED LOAD			
Load (N)	*200000*	Velocity (km/h)	*100*

4. 1. Sensitivity Analysis

Model sensitivity to certain parameters is tested in this sub-section. First of all, time discretisation for the convolution is analyzed. The values tested ranged from 0.1 to 0.001. This affects the time of calculation as well as the output accuracy. The results obtained at three different distances from the rail are shown in Figure 4 (4a at 1 meter from the track; 4b - at 6 meters; 4c - at 12 meters).

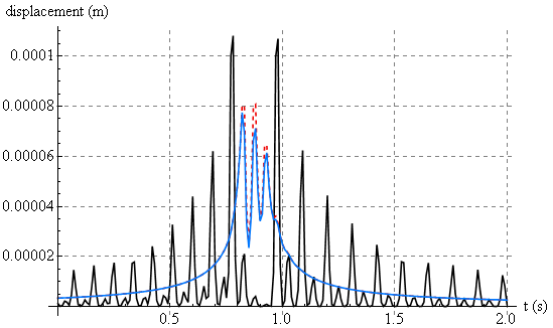

Fig. 4a. Modeled displacements at 1 meter from the track. Black→$\Delta\tau$=0.1; Dashed Red→$\Delta\tau$=0.01; Blue $\Delta\tau$=0.001

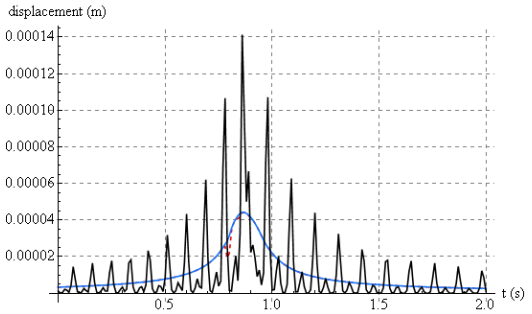

Fig. 4b. Modeled displacements at 6 meters from the track. Black→$\Delta\tau$=0.1; Dashed Red→$\Delta\tau$=0.01;Blue $\Delta\tau$=0.001

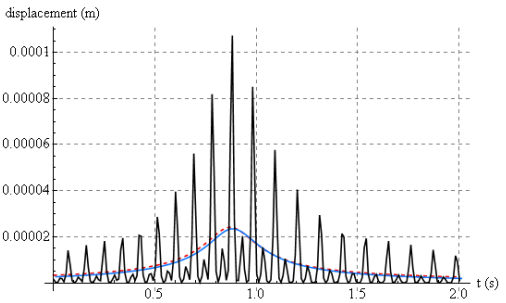

Fig. 4c. Modeled displacements at 12 meters from the track. Black→$\Delta\tau$=0.1;Dashed Red→$\Delta\tau$=0.01;Blue $\Delta\tau$=0.001

From the graphic it is clear that a discretisation of 0.1 seconds or below causes a noticeable instability in the model output. A greater discretisation is required to obtain a smoother solution closer to the expected for a single point load case. The results for a $\Delta\tau$ equal to 0.01 indicate a much steadier solution and thus this order of magnitude for discretisation is assumed to be small enough. The results for a value of 0.001 are quite similar but the time of calculation increases dramatically.

In conclusion, the time discretisation parameter, as long as it is small enough to ensure proper equivalence between a discrete and continuous convolution, has not a great effect in the model output.

Considering now the value of damping coefficients, different cases have been studied to assess the effect of these parameters in the model output. Those cases are summarized in Table 2.

Table 2. Study cases for different damping coefficients

CASE	$\mu\mu_0$ kg/m·s	$\mu\mu_1$ kg/m·s	$\mu\mu_2$ kg/m·s
1	*0*	*0*	*0*
2	*5000*	*0*	*7000*
3	*5000*	*5000*	*0*
4	*500*	*10000*	*12000*
5	*15000*	*500*	*12000*
6	*15000*	*10000*	*500*

These cases have been defined to evaluate the difference between damped and undamped soils and the effect that different order of magnitudes have in the solution. The results are shown in Figure 5, where 5a is calculated at 1 meter from the track (concrete slab); 5b - at 6 meters (soil 1) and 5c - at 12 meters (soil 2).

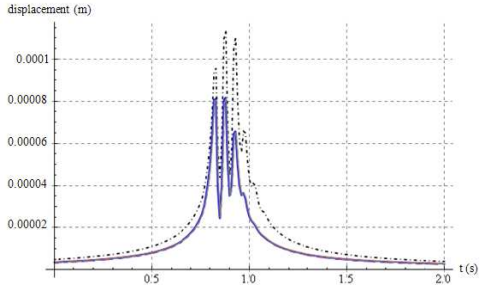

Fig. 5a. Modeled displacements at 1 meter from the track. Black=Case 1; Dashed red=Case 2; Dashed Blue=Case 3; Red=Case 4; Blue=Case 5; Gray=Case 6

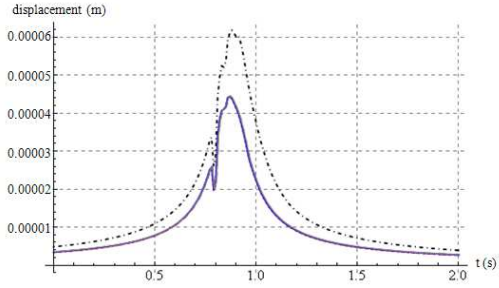

Fig. 5b. Modeled displacements at 6 meters from the track. Black=Case 1; Dashed red=Case 2; Dashed Blue=Case 3; Red=Case 4; Blue=Case 5; Gray=Case 6

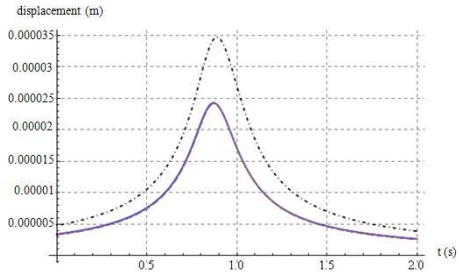

Fig. 5c. Modeled displacements at 12 meters from the track. Dashed Black=Case 1; Dashed red=Case 2; Dashed Blue=Case 3; Red=Case 4; Blue=Case 5; Gray=Case 6

From the graphics it is clear that there is a noticeable difference between case 1 (completely undamped) and the rest. The displacements modeled are higher when the parameter $\mu\mu_i$ is set to zero for the three soils. However, for the rest of the cases, variations of these parameters within the range of values considered provide almost the same solution at the three distances evaluated. This leads to conclusion that, for the range studied, any value of the parameter $\mu\mu_i$ other than zero has no direct influence in the model performance.

4. 2. Simulations

In this sub-section a whole set of simulations is carried out to assess model performance in terms of load magnitude and velocity as well as some different scenarios of track and soil typology.

First of all, different velocities are tested. The rest of the model parameters are set to the standard values detailed in Table 1. Velocities considered range from 50 to 300 km/h. The results are shown in Figure 6 (once again 6a refers to 1 meter from the track, 6b - to 6 meters and 6c - to 12 meters.).

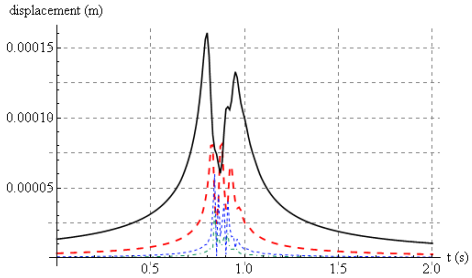

Fig. 6a. Modeled displacements at 1 meter from the track. Black→v=50 km/h; Dashed Red→v=100 km/h; Dotted Blue→v=200 km/h; Dot-Dashed Green→v=300 km/h

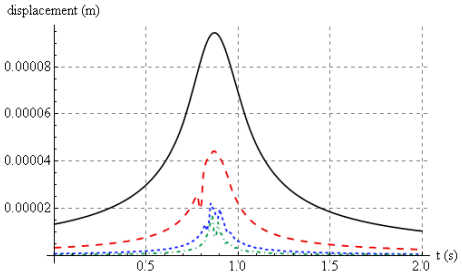

Fig. 6b. Modeled displacements at 6 meters from the track. Black→v=50 km/h; Dashed Red→v=100 km/h; Dotted Blue→v=200 km/h; Dot-Dashed Green→v=300 km/h

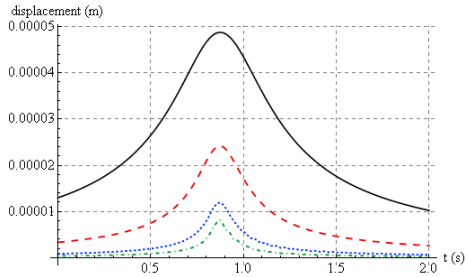

Fig. 6c. Modeled displacements at 12 meters from the track. Black→*v*=50 km/h; Dashed Red→*v*=100 km/h; Dotted Blue→*v*=200 km/h; Dot-Dashed Green→*v*=300 km/h

There is a clear influence of velocity in the modeled displacements. Lower velocities lead to higher deformations, which take place over a longer period of time. This is likely due to the damping characteristics of the materials i.e. a slower load allows the terrain to deform to a greater extent than a faster one. The gap between peaks of displacement is particularly noticeable when comparing the results for 50 and 100 km/h. The differences are much lower when comparing those for 200 and 300 km/h. On the other hand, as velocity increases the solution becomes more unsteady around the main peaks. This can be observed particularly at short distance from the track (Figure 6a) for the highest velocity (300 km/h).

Different loads are also tested, ranging from 200000 to 1000000 N. Two harmonically varying loads are also considered, both of them with an amplitude of 200000 N but with different frequencies (10 and 20 rad/s). The results are shown in Figure 7 (once again 7a refers to 1 meter from the track, 7b to 6 meters and 7c to 12 meters).

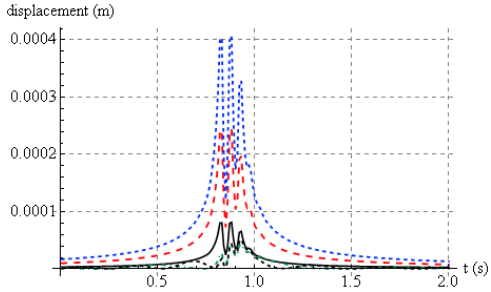

Fig. 7a. Modeled displacements at 1 meter from the track. Black→*P*=200 kN; Dashed Red→*P*=600 kN; Dotted Blue→*P*=1000 kN; Dot-Dashed Green→*P*=200 kN (f=10 rad/s); Dashed Black→*P*=200 kN (*f*=20 rad/s)

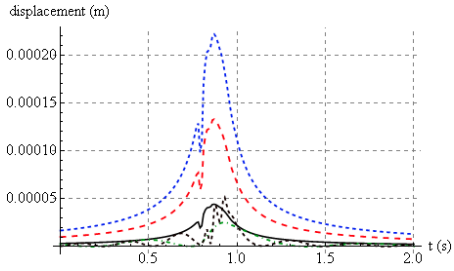

Fig. 7b. Modeled displacements at 6 meter from the track. Black→*P*=200 kN; Dashed Red→*P*=600 kN; Dotted Blue→*P*=1000 kN; Dot-Dashed Green→*P*=200 kN (f=10 rad/s); Dashed Black→*P*=200 kN (*f*=20 rad/s)

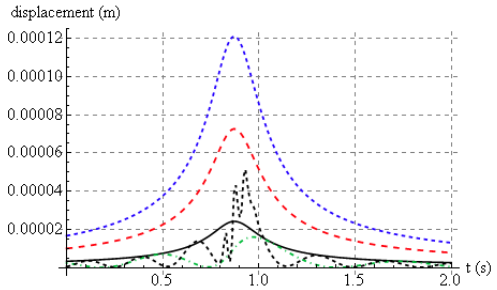

Fig. 7c. Modeled displacements at 12 meter from the track. Black→*P*=200 kN; Dashed Red→*P*=600 kN; Dotted Blue→*P*=1000 kN; Dot-Dashed Green→*P*=200 kN (*f*=10 rad/s); Dashed Black→*P*=200 kN (*f*=20 rad/s)

The more evident result is that higher loads cause higher displacements. The trend is also perfectly linear as expected from the assumption of linearity the model relies on. The most interesting conclusion comes from the harmonic loads, as it is clear than the model is capable of reproducing the displacements caused by such loads. In addition, it is observed that a harmonic load tends to cause greater peaks of deformation when compared to a constant point load of the same value. This effect depends on the load frequency: The higher it is, the higher the peak of displacement is given by the model.

Finally, different combinations of materials are studied with the model. Four cases are defined as shown in Table 3.

Table 3. Study cases for different materials

CASE	SLAB	SOIL 1	SOIL 2	DESCRIPTION
1	ρ_0=2400 μ_0=14E8 $\mu\mu_0$=15000	ρ_0=1500 μ_0=5E7 $\mu\mu_0$=2000	ρ_0=1800 μ_0=18E7 $\mu\mu_0$=7000	Less competent slab/soil 1
2	ρ_0=2400 μ_0=14E8 $\mu\mu_0$=15000	ρ_0=1500 μ_0=5E7 $\mu\mu_0$=2000	ρ_0=2400 μ_0=14E8 $\mu\mu_0$=15000	Less competent soil 1
3	ρ_0=2400 μ_0=14E8 $\mu\mu_0$=15000	ρ_0=2200 μ_0=12E8 $\mu\mu_0$=12000	ρ_0=1500 μ_0=5E7 $\mu\mu_0$=2000	Less competent soil 2
4	ρ_0=1800 μ_0=7E7 $\mu\mu_0$=2000	ρ_0=1830 μ_0=18E7 $\mu\mu_0$=5000	ρ_0=2000 μ_0=14E8 $\mu\mu_0$=7000	Less competent slab

The rest of the parameters are set to the values detailed in Table 1. The results obtained for these 4 cases are shown in Figure 8.

In the first graphic (8a, 1 meter from the track) one can observe that the greater displacements are obtained for case 2. Case 1 provides a first peak quite close to that established for case 2 but the rest of the peaks are clearly smaller. This is likely due to the difference of stiffness between soil 1 and 2 in both cases: In case 2 the second soil is far more rigid than the first one and, thus, there is more wave reflection towards the track, hence explaining the increase of displacement. In case 1, as the two soils are more similar, there is more energy transmitted and less reflected.

It is also noticeable that the peaks for case 4 are smaller than those for case 1 and 2, despite having a less rigid slab. This means that the displacements modeled in a spot close to the track

are more influenced by the characteristics of the two soils than those of the slab itself. As for case 3, a negative peak is found, which could be due to the high rigidity of the slab and the soil 1: As the wave deforms soil 1, this layer affects the slab and pulls it up, hence giving a negative displacement (see Figure 1 for the axis considered in the model).

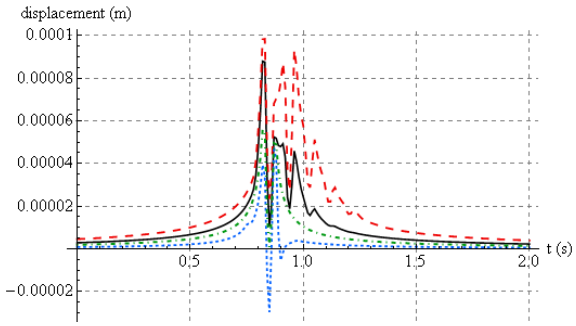

Fig. 8a. Modeled displacements at 1 meter from the track. Black→Case 1; Dashed Red→ Case 2; Dotted Blue→Case 3; Dot-Dashed Green→Case 4

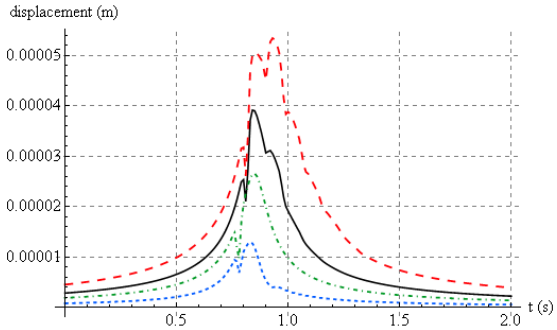

Fig. 8b. Modeled displacements at 6 meter from the track. Black→Case 1; Dashed Red→ Case 2; Dotted Blue→Case 3; Dot-Dashed Green→Case 4

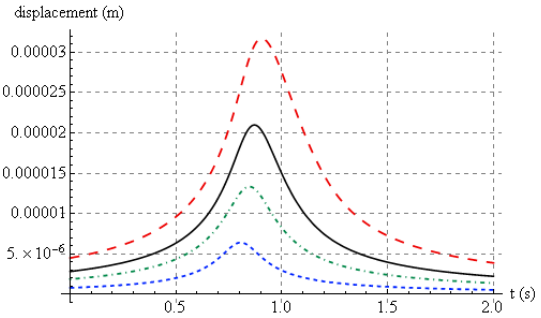

Fig. 8c. Modeled displacements at 12 meter from the track. Black→Case 1; Dashed Red→ Case 2; Dotted Blue→Case 3; Dot-Dashed Green→Case 4

The second and third graphics (8b at 6 meters from the track, 8c at 12 meters) reveal similar trends: the highest peaks are observed for cases 2 and 1 respectively, which confirms the great influence that the soil 1 has over the rest of the model domain. Another conclusion can be drawn from Figure 8b, where the displacements are higher in case 4 than in case 3. This implies that the displacements in soil 1 are more affected by the slab than by the soil 2.

As an overall conclusion, it can be said that the best configuration in terms of lower peaks of displacement is that of case 3, i.e. a more rigid slab and soil 1 regardless of the characteristics of soil 2. This configuration, however, may cause negative displacements in the slab that should be taken into account.

4. CONCLUSIONS

The model developed and presented in this study is an analytical one and is capable of reproducing the propagation of vibrations (in terms of displacements) from the track itself through the surface of the surrounding soil. The model considers a single point load with a either constant or harmonically varying magnitude, which moves along the track at a constant speed. It is formulated to take into account phenomena such as wave scattering and wave reflection in the interfaces between different materials.

The model is, at this stage, fully theoretical. The simulations carried out in this paper demonstrate many of its possibilities in terms of evaluating factors such as load magnitude or velocity and testing different track and soil configurations. Therefore, it can be considered as a useful tool to study the phenomenon of vibration propagation from railway infrastructures from a theoretical point of view.

There are, however, certain aspects of the model that could be improved in future stages of research so as to turn it into an instrument for engineers and track designers. So far the model takes a single point load as an input, but this can be expanded to include a set of loads, which better represent the passing of a train with several axles. As for the load magnitudes, they could be modified to consider not only the static load due to the train weight but also include dynamic loads caused by rail and wheel defects.

With these improvements the model could be compared with real data in order to calibrate some of its parameters. The model would be therefore validated to be used as a reliable tool for decision-making.

REFERENCES

[1] Thompson D. J. Railway Noise and Vibration: Mechanisms, Modelling and Means. Oxford: Elsevier, 2009.

[2] Galvín P., Domínguez J. Analysis of ground motion due to moving surface loads induced by high-speed trains. Engineering Analysis with Boundary Elements, Vol. 31, Issue 11, 2007, p. 931–941.

[3] Metrikine A. V., Vrouwenvelder A. C. W. M. Surface ground vibration due to a moving train in a tunnel: two-dimensional model. Journal of Sound and Vibration, Vol. 234, Issue 1, 2000, p. 43–66.

[4] Salvador P., Real J., Zamorano C., Villanueva A. A procedure for the evaluation of vibrations induced by the passing of a train and its application to real railway traffic. Mathematical and Computer Modelling, Vol. 53, Issue 1-2, 2010, p. 42-54.

[5] Real J., Martínez P., Montalbán L., Villanueva A. Modelling vibrations caused by tram movement on slab track line. Mathematical and Computer Modelling, Vol. 54, Issue 1-2, 2011, p. 280-291.

[6] Sheng X., Jones C. J. C., Thompson D. J. Prediction of ground vibration from trains using the wavenumber finite and boundary element methods. Journal of Sound and Vibration, Vol. 293, Issue 3-5, 2006, p. 575–586.

[7] Yang Y. B., Hung H. H. Soil vibrations caused by underground moving trains. Journal of Geotechnical and Geoenvironmental Engineering, Vol. 134, Issue 11, 2008, p.1633-1644.

[8] Celebi E. Three-dimensional modeling of train-track and sub-soil analysis for surface vibrations due to moving loads. Applied Mathematics and Computation, Vol. 179, Issue 1, 2006, p. 209–230.

[9] Katou M., Matsuoka T., Yoshioka O., Sanada Y., Miyoshi T. Numerical simulation study of ground vibrations using forces from wheels of a running high-speed train. Journal of Sound and Vibration, Vol. 318, Issue 4-5, 2008, p. 830-849.

[10] Koziol P., Mares C., Esat I. Wavelet approach to vibratory analysis of surface due to a load moving in the layer. International Journal of Solids and Structures, Vol. 45, Issue 7-8, 2008, p. 2140–2159.

[11] Andersen L., Nielsen S. R. K. Reduction of ground vibration by means of barriers or soil improvement along a railway track. Soil Dynamics and Earthquake Engineering, Vol. 25, Issue SI, 2005, p. 701-716.
[12] Dawn T. M., Stanworth C. G. Ground vibrations from passing trains. Journal of Sound and Vibration, Vol. 66, Issue 3, 1979, p. 355-362.
[13] Gutowski T. G., Dym C. L. Propagation of ground vibration - Review. Journal of Sound and Vibration, Vol. 49, Issue 2, 1976, p. 179-193.
[14] Sheng X., Jones C. J. C., Petyt M. Ground vibration generated by a load moving along a railway track. Journal of Sound and Vibration, Vol. 228, Issue 1, 1999, p. 129-156.
[15] Jones C. J. C., Sheng X., Petyt M. Simulations of ground vibration from a moving harmonic load on a railway track. Journal of Sound and Vibration, Vol. 231, Issue 3, 2000, p. 739-751.
[16] Auersch L. The excitation of ground vibration by rail traffic: theory of vehicle–track–soil interaction and measurements on high-speed lines. Journal of Sound and Vibration, Vol. 284, Issue 1-2, 2005, p. 103–132.
[17] Barber J. R. Surface displacements due to a steadily moving point force. Journal of Applied Mechanics, Vol. 63, Issue 2, 1996, p. 245-251.
[18] Udías A. Principles of Seismology. Cambridge: Cambridge University Press, 1999.
[19] Tijonov A. N., Samarsky A. A. Equations of Mathematical Physics. Moscow: Mir, 1980.